

promoting access to White Rose research papers



Universities of Leeds, Sheffield and York
<http://eprints.whiterose.ac.uk/>

This is an author produced version of a paper published in **Engineering Fracture Mechanics** .

White Rose Research Online URL for this paper:

<http://eprints.whiterose.ac.uk/9201/>

Published paper

Yates, J.R., Zanganeh, M., Tomlinson, R.A., Brown, M.W. and Garrido, F.A.D. (2008) *Crack paths under mixed mode loading*. Engineering Fracture Mechanics, 75 (3-4). pp. 319-330.

<http://dx.doi.org/10.1016/j.engfracmech.2007.05.014>

Crack paths under mixed mode loading

J.R Yates¹, M. Zanganeh², R.A. Tomlinson³, M.W. Brown⁴ and F.A. Diaz Garrido⁵

¹j.yates@sheffield.ac.uk, Department of Mechanical Engineering, The University of Sheffield, S1 3JD, UK

²m.zanganeh@sheffield.ac.uk

³r.a.tomlinson@sheffield.ac.uk

⁴m.brown@sheffield.ac.uk

⁵fdiaz@ujaen.es, Departamento de Ingeniería Mecánica y Minera, Universidad de Jaen, Spain.

ABSTRACT.

Long fatigue cracks that initially experience mixed mode displacements usually change direction in response to cyclic elastic stresses. Eventually the cracks tend to orient themselves into a pure mode I condition, but the path that they take can be complex and chaotic. In this paper we report on recent developments in techniques for tracking the crack path as it grows and evaluating the strength of the mixed mode crack tip stress field.

KEYWORDS

Fatigue crack growth, thermoelastic stress analysis, stress intensity factor, interacting fatigue cracks

INTRODUCTION

There are many opportunities for cracks and crack-like defects in engineering structures to exist in orientations that induce mixed mode crack tip displacements. Defects arising from fabrication processes such as welding or casting; cracks created under the action of residual tensile stresses; cracking of embrittled microstructures; and fatigue cracks that have grown under the action of some previously applied loading cycles that differ from the current load case can all create flaws with some arbitrary combination of mode I, II and III stress intensities.

In this paper we present the results of experiments using thermoelastic stress analysis to study interacting mode I cracks. We also compare the cyclic stress intensity factors obtained from these experiments with numerical simulations using finite element analysis packages.

Broberg [1] discussed aspects of the stability of the crack path under pure and mixed mode loads and concluded that crack paths remain straight under homogeneous remote stress fields. However, engineering structures in service rarely experience such well defined uniform stress fields. Stress and strain gradients arising from geometric features, multiple cracks and non-uniform, non-proportional remote loads commonly occur.

Applied mixed mode loading and interaction between multiple cracks are the principal causes of a major loss of directional stability. Highly anisotropic

microstructures can also lead to significant changes in crack orientation but more often are responsible for local deviations, or ‘zigzags’, in the overall mode I crack trajectory.

Broberg also noted that the ideal mode I elastic crack tip stress field did not provide a sufficient condition for cracks to maintain a straight path. It was proposed, from the work of Rice *et al.* [2] and Anderson [3], that it is the plastic flow at the crack tip that dictates the crack path. The notion that the crack path is governed by the plastic behaviour of the crack tip is supported by many workers. Under mode III loading, the propensity for flat, or shear, mode growth is strongly influenced by the plastic part of the crack tip displacement. Plumbridge [4] performed experiments on aluminium plates cyclically loaded under Mode III loading conditions. It was observed that when the crack tip plastic zone is large in comparison with the plate thickness crack extension proceeds by a valid Mode III mechanism. When the crack tip plasticity is small and restricted to planes of maximum shear there is a strong component of Mode I cracking which results in delamination in the direction of macroscopic growth. In torsional fatigue, the extent of crack tip plasticity plays an important role in governing whether the crack path is flat or faceted [5, 6]. Extensive crack tip plasticity will encourage the formation of a flat, shear mode fracture surface over the faceted, or ‘factory roof’, surface observed under essentially linear elastic conditions.

The shape of the plastic zone under pure mode III conditions differs substantially from the shape ahead of a mode I crack. In mode III, the plastic zone is essentially circular and extends some four to six times further ahead of the crack than the symmetrical inclined shear distribution seen ahead of a pure mode I crack at the same

stress intensity factor. The centre of the circular plastic zone lies somewhere between the tip of the crack and one radius distance ahead, depending on the work hardening coefficient [7-10].

Furthermore, the extent of crack tip plasticity in torsional loading, and hence the prevalence of flat mode growth, is also dependent upon the size of the cylindrical component [11,12]; small diameter shafts being more prone to flat crack growth than large shafts for the same stress, or strain, intensity factor. In these cases, a large ratio of the applied torque to the plastic collapse limit torque of the shaft, as would occur in a small diameter shaft, extends the crack tip plasticity beyond that expected for the level of strain intensity factor applied.

Under mixed mode I+III, an increasing mode III contribution is known to lead to an increase in the concentration of the plastic strain in the trajectory of the crack [13] as the plastic zone changes from the twin lobed mode I shape to the circular mode III configuration, as shown in Figure 1 [14].

The shear *versus* branch crack competition is probably most apparent under sequential cyclic mode I and mode II loads, as experienced in cracked railway lines. The evidence for the role of the crack tip plasticity in preventing the crack from branching into the pure mode I trajectory in this case is overwhelming [15].

The path of a fatigue crack under proportional loading from an initially mixed mode condition, as created by angled or inclined cracks in laboratory specimens, is surprisingly stable. One might expect major variations, as a function of mean stress for example, but there is little evidence to this effect. Nevertheless, there are subtle

differences in the crack trajectory in specimens under identical test conditions. These small scale fluctuations in crack path are worthy of detailed investigation but, until recently, experimental techniques to evaluate the strength of mixed mode crack field have not been precise or reliable enough to yield useful information.

Understanding the behaviour of mixed mode cracks in general, and the path of such cracks in particular, requires a combination of high quality experimental data and observations as well as robust physically based models. Good data on the crack tip stress state, crack closure and contact, and the crack trajectory is hard to obtain and there has been much recent work in this area.

In this paper, we set out to report on some recent developments in gathering experimental data on mixed mode stress and displacement fields. We also consider how such techniques might provide an opportunity to investigate issues surrounding the stability of crack paths in varying stress fields.

OVERVIEW OF FULL FIELD TECHNIQUES FOR CRACK ANALYSIS

Photoelasticity, moiré interferometry, electronic speckle pattern interferometry (ESPI), image correlation and thermoelasticity, or differential thermography, are all techniques which provide full field experimental data on crack tip displacements or strains. From these data, crack tip stresses can be inferred and hence stress intensity factors derived. With the advent of advanced computing power and digital image processing, techniques such as photoelasticity and moiré interferometry have moved from slow manual

methods where fringe orders must be identified and located by an experienced operator, to those where stress intensity factors may be determined in a matter of minutes.

Fracture mechanics studies using transmission photoelasticity require fine slits to be introduced into epoxy models of engineering components [16, 17]. Several methods have been developed to determine K_I and K_{II} using the full field of data surrounding the slit tip [18, 19]. Nurse and Patterson [16] also developed a photoelastic method to predict the direction of crack growth using the theory that long cracks usually grow under mode I loading in direction perpendicular to maximum tangential stress. They found that when K_{II}/K_I is less than 0.7, this direction is approximately equivalent to the axis of symmetry observed in the isochromatic fringes loops and so one can predict the direction of crack growth. This method was further developed by Burguete and Patterson [20] to investigate the effect of friction on crack propagation in the dovetail fixings of gas turbine compressor discs.

Nurse and Patterson [21] used reflection photoelasticity to study a fatigue crack in an aluminium alloy using a stroboscopic light source over the complete load cycle. However the drawback to this method is the fact that the birefringent coating must not cover the crack and thus the crack growth direction must be predicted before applying the coating. Further investigations of fatigue crack closure were made by Pacey *et al.* [22], using transmission photoelasticity through a polycarbonate specimen, which is known to undergo stable fatigue crack growth. A method to evaluate mixed mode stress intensity factors was developed based on the Muskhelishvili stress field formulation together with a genetic algorithm and the downhill simplex method. This numerical

optimisation procedure was found to offer a significant advance in the ability to characterise the behaviour of fatigue cracks with plasticity induced crack closure.

Similar studies on mixed mode fatigue crack propagation have been carried out using geometric moiré [23] and moiré interferometry [24]. Moiré methods are particularly useful when making high temperature measurements [25]. Moiré interferometry involves bonding a fine grating ahead of the crack tip. In the past these tended to debond due to the high strain gradients in that area, but the recent development of photoresist methods allows the production of well-adhered gratings of $0.75\mu\text{m}$ thickness [26]. It now means that fatigue cracks can grow through the grating and allow detailed crack closure investigations to be carried out [27].

When studying fatigue crack propagation it is desirable to be able to evaluate the stress intensity factor range of the growing crack. To do so, the techniques based on photoelasticity and interferometry require data to be collected at maximum and minimum load. This can be done in several ways. Firstly, the cycling can be stopped at the required loads and data taken under static conditions. Alternatively, the component can be illuminated by a stroboscopic light synchronised with some part of the fatigue cycle. The development of modern high speed digital video cameras means that data can be collected at several points in the loading cycle and the changing stress field determined throughout the cycle.

Differential thermography, or Thermoelastic Stress Analysis (TSA), has proved to be an invaluable tool to explore the crack tip strain field during fatigue loading [28-31]. When a material is subject to cyclic strain under adiabatic conditions, an asynchronous

cyclic temperature variation occurs on its surface which is directly proportional to the first strain invariant. In thermoelastic stress analysis, this temperature variation is measured using very sensitive infra-red detectors and processed to provide a map of the surface stress distribution. When the mixed mode stress field around a fatigue crack is examined, see Figure 2, the temperature data from the elastic field around the crack tip can be used to evaluate the range of both ΔK_I and ΔK_{II} . A number of methodologies for calculating the stress intensity factor are available and have been reviewed by Tomlinson and Olden [32] in 1999. More recently, developments have focussed on greater accuracy in the determination of mixed-mode stress intensity factors [33-35].

Historically, analysis of the data required knowledge of the location of the crack tip and an initial estimate of the stress intensity factor. Further developments of the TSA technique [36, 37] provided a means of both tracking the location of the crack tip during propagation under cyclic loading and determining the stress intensity factor range *a priori*. Figure 3 shows the tracking of a crack growing from a 45° notch under tensile loading.

Extracting the elastic stresses from around the growing crack tip provides a good estimate of, what is often called, the effective stress intensity factor range. In reality, this is the true stress field experienced by the crack, rather than the nominal, or applied ΔK . Thermoelastic stress analysis, therefore, provides a method for estimating the crack closure levels directly.

In the last few years, Electronic Speckle Pattern Interferometry (ESPI) and image correlation have been used to measure crack tip displacements and strains. Shterenlikht

et al. [38] developed the method used in photoelasticity by Nurse and Patterson [19] to accurately determine mixed-mode stress intensity factors using full field ESPI and image correlation data. An advantage of these techniques is that minimal specimen preparation is required, only using the painted or abraded surface of the component, unlike reflection photoelasticity and moiré where a coating or grating has to be bonded to the surface. The latest developments [39] in image correlation can provide information on the crack position and the crack tip displacement field.

EXPERIMENTAL PROCEDURE

Offset double edge slit fatigue specimens (Figure 4) were used to explore the trajectory and crack tip stress states of a pair of interacting fatigue cracks. Specimens 6 mm thick, 40 mm wide and 250 mm long were machined from a plate of 7010 T7651 aluminium alloy. Two slits, each 8 mm long and on opposite sides of the specimens, were electric discharge machined using 0.3 mm diameter wire. The vertical offset between the two slits were chosen to be 0, 8, 16, 32 and 48 mm for the series of tests conducted. One face of each specimen was painted with a thin coat of matt black paint (RS type 496-782) to provide a surface of uniform and known emissivity. A single rosette strain gauge (Tokyo Sokki Kenkyujo Co., 1 mm, $120 \pm 0.5 \Omega$) was bonded to the specimen in a region of uniform and known elastic stress to provide a calibration for the thermoelastic data.[29]

Specimens were loaded through two pins located 210 mm apart. Fatigue tests were conducted under load control at a frequency of 20 Hz, a range of 3.6 kN and a mean

load of 14.4 kN for the 0 and 8 mm offset specimens and a range of 3.5 kN and a mean load of 8.5 kN for the remaining three specimens. The load range was reduced since considerable plasticity was observed in the first two tests. The frequency was chosen to be sufficiently high for adiabatic conditions to be attained in the material ahead of the crack tip. By doing so, we ensured that the thermoelastic signal contains information about the sum of the elastic principal stresses from which the mode I and mode II stress intensity factor ranges can be evaluated.

A Deltatherm 1550 instrument manufactured by Stress Photonics Inc. was used to gather thermoelastic data from the matt black surface. The crack tip position and the mode I and mode II stress intensity factor ranges occurring in the specimen were evaluated using the FATCAT software [40].

The FRANC2DL finite element package [41] was used to predict the likely path of the cracks for each of the offset conditions. The stress intensity factor can be determined using the J integral method, the displacement correlation technique and the modified crack closure technique in FRANC2DL. Also, to predict the crack path three different criteria can be applied. Those are the maximum tangential stress, the maximum energy density factor and the minimum energy release rate criterion. The predicted trajectory varies slightly according to the method used in the calculation of stress intensity factors and the crack turning criterion chosen. Although there are no major discrepancies, there are small differences in the crack paths predicted, especially in the case where the cracks are initially only slightly offset. The paths found by using the

maximum tangential stress turning criterion and displacement correlation was used to evaluate the stress intensity factors.

RESULTS AND DISCUSSION

A qualitative comparison between the thermoelastic and finite element data is made in Figure 5. The experimental crack paths are very similar to those predicted by the finite element method. This is relatively surprising since the numerical simulations assume that both the left and right hand cracks start growing at the same time. In practice, the creation of a growing fatigue crack from the tip of the spark machine slit takes a different number of cycles in every case, and the cracks do not grow symmetrically as can be observed in the thermoelastic data from the 0 mm offset in Figure 5.

Quantitative comparisons are made in Figures 6 and 7. The crack tip positions throughout the tests were located from the thermoelastic data and compared with the positions predicted by the FRANC2DL finite element package for offsets of 0, 16 and 48 mm respectively in Figure 6.

The values of ΔK_I derived from the FRANC2DL analysis, Figure 7, are broadly consistent with the experimental results. The best agreement is for the dominant crack; that is the one that started first and grew faster. The second crack tended to have a lower stress intensity range than predicted from the numerical modelling.

In the early stages of crack growth the cracks followed the path where the mode II stress intensity factor is practically zero. However, there are some regions, shown in Figure 8,

where a significant mode II stress intensity factor is noticeable. It is exactly in these regions where the deviation of the predicted crack paths from the experimental crack path is observed.

As can be observed in the TSA image in Figure 9(a) there are regions on the crack flanks where non-uniform stresses appear, which could be due to contact between the crack faces. Therefore the possibility of crack face contact and the extent of plasticity at the crack tip were explored using non-linear finite element analysis. An elastic plastic finite element model was developed in ANSYS® [42] which reproduced the crack path observed experimentally. A fine mesh using 8 node elements was used to model the region ahead of crack tip and a bihardening model was used for material behaviour modelling. In Figure 9(b) are presented the sum of principal strains in the specimen obtained from FE analysis. As is well known, the sum of principal strains is proportional to the thermoelastic signal. By comparing the two Figures 9(a) and 9(b) it can be seen that the results from the finite element analysis show a very similar pattern of dilatational strain, particularly in areas along the crack flanks. Since the numerical model showed that there was no contact between the crack faces, it is concluded that the strains, and hence stresses, observed on the crack flanks were due to bending of the ligament of material between the two cracks. Examination of the fracture surface, Figure 10, does not show any evidence of crack face contact or rubbing and confirms this conclusion.

Although the sum of the principal strains in both images in Figure 9 are similar in the crack tip region, it seems that the contours in the TSA image around the crack tip have

twisted from the crack plane more than is observed in the FE analysis. This was investigated by observing the fracture surfaces as it was suspected to be due to crack tunnelling. When the fracture surface was examined, shear lips were observed at the end of crack growth (Figure 10) which indicated a transition from tensile to shear fracture in the region where the plastic strains increase significantly. These coincide exactly with the point where the crack path deviated from the modelling predictions and where the high values of ΔK_{II} were observed. It is recognised that three-dimensional modelling would provide further insight into the crack propagation and work has begun using this approach. The fact that only surface data may be recorded is a limitation of the thermoelastic technique, but no other non-destructive techniques can monitor the internal crack front as it propagates. Modern thermoelastic apparatus used here allows data collection in near real time, which offers the potential of using experimental and numerical techniques together from which valuable information can be obtained. From these experiments it appears that the elastic stress field, as characterised by the stress intensity factor, may be only partially controlling the crack path. If Broberg's assertion is correct, and it is the directionality of the plastic strain field that governs the crack path, then we should be seeking ways of measuring plastic strains directly. It is suggested that the latest developments in image correlation techniques [39] and differential thermography may provide a route to quantitative evaluation of the non-linear strains fields around a crack tip and hence offer some further insight into the trajectory of fatigue cracks.

CONCLUSIONS

Recent developments in experimental mechanics offer an opportunity to explore the hypothesis that the direction of fatigue cracks may be governed more strongly by directionality of crack tip plasticity rather than by the magnitude of the elastic stress field alone.

REFERENCES

- [1] Broberg K.B., 1987. On crack paths. *Engng Fracture Mech.* **28**, 663-679.
- [2] Rice J.R., Drugan W.L., Sham T.L., 1980. Elastic plastic analysis of growing cracks. In: Wheeler J.B. (Ed.), *ASTM STP 700, Fracture Mech.* ASTM, 1980. pp. 189-221.
- [3] Andersson H., 1977. Analysis of a model for void growth and coalescence ahead of a moving crack tip. *J Mech Phys Solids* **25**, 217-233.
- [4] Plumbridge W.J., 1985. Fatigue crack growth in plate specimens under Mode III loading. *J Mater Sci.* **20**, 1015-1026.
- [5] Hay E., Brown M.W., 1986. Initiation and early crack growth of fatigue cracks from a circumferential notch loaded in torsion. In: Miller K.J., de los Rios E.R. (Eds), *The Behaviour of Short Fatigue Cracks.* MEP Ltd. London, 1986. pp. 309-321

- [6] Nayeb-Hashemi H., McClintock F.A., Ritchie R.O., 1982. Effects of friction and high torque on fatigue crack propagation in mode III. *Met Trans A.* **13A**, 2197-2204.
- [7] Rice J.R., 1967. Stresses due to a sharp notch in a work-hardening elastic plastic material loaded by longitudinal shear. *J. App. Mech.* **34**, 287-298.
- [8] Weertman J., 1989. Mode III crack tip plastic zone solution for work hardening solid using dislocation motion. *J. App. Mech.* **56**, 976-977.
- [9] Weertman J., 1991. Complete crack-tip shielding of the Mode III crack in a work hardening solid. *J. App. Mech.* **58**, 1107-1108.
- [10] Zacharopoulos N., Srolovitz D., LeSar R., 2003. Discrete dislocation simulations of the development of a continuum plastic zone ahead of a stationary mode III crack. *J. Mech. Phys. Solids* **51**, 695-713.
- [11] Tschegg E.K., 1983. Mode III and mode I fatigue crack propagation behaviour under torsional loading. *J Mater Sci.* **18**, 1604-1614.
- [12] Yates J.R., 1987. Crack tip plastic zone sizes in cylindrical bars subjected to torsion. *Fatigue Fract Engng Mater Struct.* **10**, 471-477.
- [13] Kamat S.V., Srinivas M., 2001. Effect of mixed mode I/III loading on plastic zone in Armco Iron. *Materials Science and Technology* **17**, 1163-1165.
- [14] Yates J.R., 1987. Fatigue under combined torsion and bending loads. PhD thesis, University of Sheffield, UK.
- [15] Bold P.E., Brown M.W., Allen R.J., 1991. Shear mode crack growth and rolling contact fatigue. *Wear* **144**, 307-317.

- [16] Nurse A.D., Patterson E.A., 1993. Experimental determination of stress intensity factors for cracks in turbine discs. *Fatigue Fract. Engng Mater. Struct.* **16**, 315-325.
- [17] Hobbs J., Burguete R., Heyes P., Patterson E.A., 2001. A photoelastic analysis of crescent-shaped cracks in bolts. *J. Strain Anal. Engng Design* **36**, 93-99.
- [18] Paris F., Picon R., Marin J., Canas J., 1996. Photoelastic determination of KI and KII: a numerical study on experimental data. *Exp. Mech.* **37**, 45-55.
- [19] Nurse A.D., Patterson E.A., 1993. Determination predominantly Mode II stress intensity factors from isochromatic data. *Fatigue Fract. Engng Mater. Struct.* **16**, 1339-1354.
- [20] Burguete R.L., Patterson E.A., 1998. The effect of friction on crack propagation in the dovetail fixings of compressor discs. *Proc. I .Mech. E., Part C* **212**, 171-181.
- [21] Nurse A.D., Patterson E.A., 1994. Photoelastic measurement of stress intensity factors during a complete fatigue cycle. In: Gomes S. (Ed.), *Recent Adv. Exp. Mech.*, Taylor and Francis, 1994. pp. 195-199
- [22] Pacey M.N., James M.N., Patterson E.A., 2005. A new photoelastic model for studying fatigue crack closure. *Exp. Mech.* **45**, 42-52.
- [23] Han M.K., Carlsen C.A., Ramulu M., 2005. Mixed mode fatigue crack propagation in 7075 T6 aluminium sheet material. In: *Advances in Fracture and Strength. Parts 1-4. Key Engineering Materials 297-300*, 2005, pp. 1565-1571
- [24] Kokaly M.T., Lee J., Kobayashi A.S., 2003. Moiré interferometry for dynamic fracture study. *Optics Lasers Engng.* **40**, 231-247.

- [25] Tran D.K., Kobayashi A.S., White K.W., 2001. Crack growth in alumina at high temperature. *Engng Fract. Mech.* **68**, 149-161.
- [26] Fellows L.J., Gungor S., 1998. Fabrication of photoresist diffraction gratings on Ti6Al4V beam specimens for use in moiré interferometry. *Meas. Sci. Tech.* **9**, 1963-1968.
- [27] Fellows L.J., Nowell D., 2005. Measurement of Crack closure after the application of an overload cycle using moiré interferometry. *Int. J. Fatigue* **27**, 1453-1462.
- [28] Lesniak J.R., Bazile D.J., Boyce B.R., Zickel M.J., Cramer K.E., Welch C.S., 1996. Stress intensity measurement via infra-red focal plane array. In: ASTM STP 1318, ASTM, 1996. pp. 208-220
- [29] Tomlinson R.A., Nurse A.D., Patterson E.A., 1997. On determining stress intensity factors for mixed-mode cracks from thermoelastic data. *Fatigue Fract. Engng Mater. Struct.* **20**, 217-226.
- [30] Lin S.T., Feng Z., Rowlands R.E., 1997. Thermoelastic determination of stress intensity factors in orthotropic composites using the J-integral. *Engng Fract. Mech.* **56**, 579-592.
- [31] Fulton M.C., Dulieu-Barton J.M., Stanley P., 1998. Improved evaluation of stress intensity factors from SPATE data. In: Allison I.M. (Ed.), *Proc. 11th Int. Conf. Exp. Mech.*, Netherlands, 1998, pp. 1211-1216
- [32] Tomlinson R.A., Olden E.J., 1999. Thermoelasticity for the analysis of crack tip stress fields - a review. *Strain* **35**, 49-55.

- [33] Marsavina L., Tomlinson R.A., 2004. Thermoelastic investigations for fatigue life assessment. *Exp. Mech.* **44**, 487-494.
- [34] Dulieu-Barton J.M., Worden K., 2003. Genetic identification of crack-tip parameters using thermoelastic isopachics. *Measurement Science and Technology* **14**, 176-183 and erratum 1845.
- [35] Diaz F.A., Patterson E.A., Tomlinson R.A., Yates J.R., 2004. Measuring stress intensity factors during fatigue crack growth using thermoelasticity. *Fatigue Fract. Engng Mater. Struct.* **27**, 571-584.
- [36] Diaz F.A., Yates J.R., Patterson E.A., 2004. Some improvements in the analysis of fatigue cracks using thermoelasticity. *Int. J. Fatigue* **6**, 365-376.
- [37] Diaz F.A., Patterson E.A., Yates J.R., 2005. Differential thermography reveals crack tip behaviour. In: *Proc. 2005 SEM Annual Conf. on Exp. App. Mech.*, Society for Experimental Mechanics, 2005, pp. 1413-1418
- [38] Shterenlikht A., Diaz Garrido F.A., Lopez Crespo P., Withers P.J., Patterson E.A., 2004. Mixed Mode (KI + KII) Stress intensity factor measurement by Electronic Speckle Pattern Interferometry and Image Correlation. In: *Proc BSSM Int. Conf. on Adv. Exp. Mech.*, BSSM, 2004. CD Rom
- [39] López-Crespo P., Shterenlikht A., Yates J.R., Patterson E.A. and Withers P.J., 2006. Crack monitoring around a hole under mixed mode (I+II) loading by image correlation. In: *Proc. Int. Conf. on Crack Paths (CP2006)*, Parma, Italy.

- [40] Diaz Garrido F.A., 2004. Development of a methodology for thermoelastic investigation of the effective stress intensity factor. PhD thesis, University of Sheffield, UK.
- [41] James M., Swenson D., FRacture ANalysis Code 2-D/Layered
<http://www.mne.ksu.edu/~franc2d>
- [42] <http://www.ansys.com>.

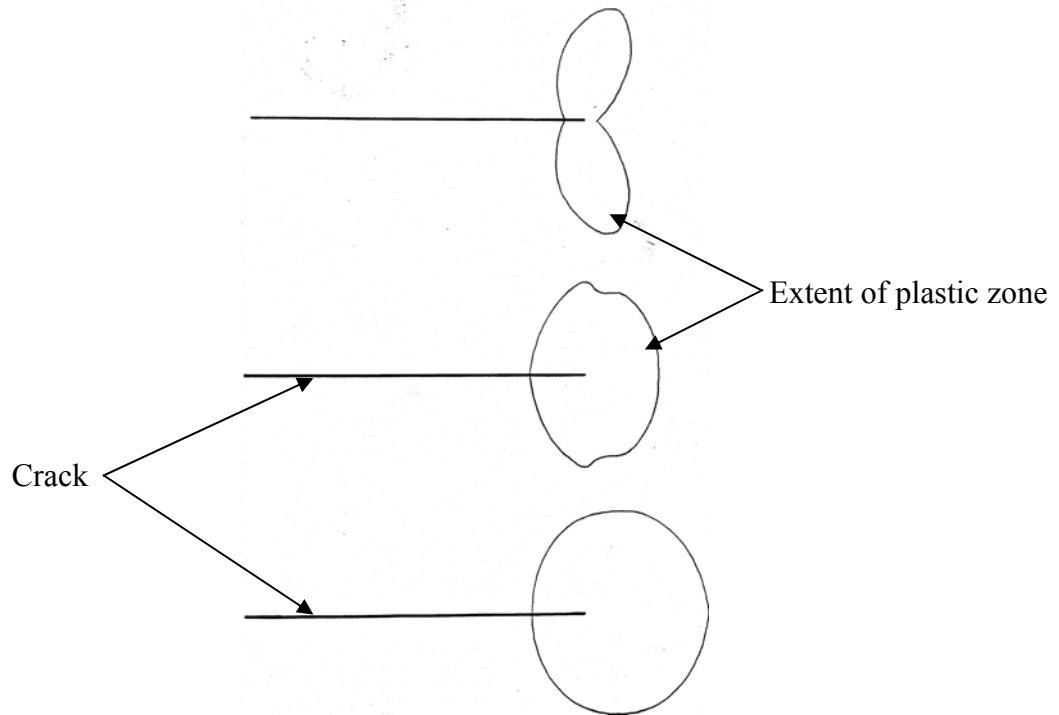


Figure 1. Changes in plastic zone shape from pure mode I (top), through $K_I/K_{III} = 1.5$ (middle), to $K_I/K_{III} = 0.5$ (bottom) from [14].

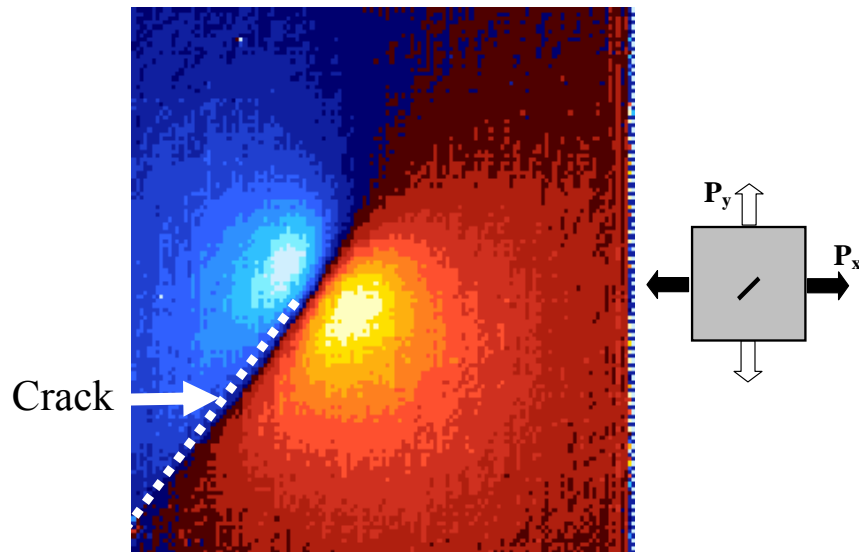


Figure 2. Typical map of thermoelastic signal around a mixed mode I+II crack tip under biaxial load, applied $\Delta K_{II}/\Delta K_I = 2$, from [40]. The signal is directly proportional to $\sigma_1 + \sigma_2$.

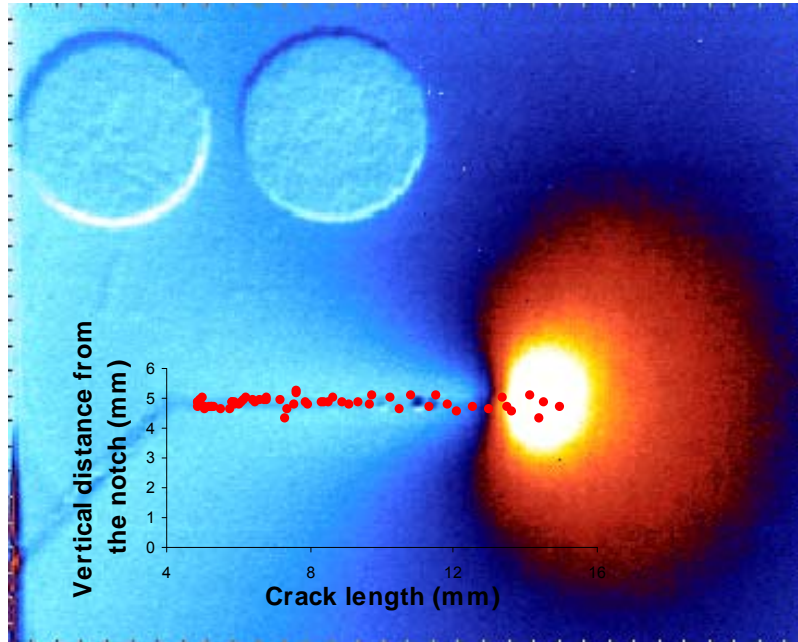


Figure 3. Tracking of a crack during fatigue cycling of a ferritic steel using differential thermography, from [40].

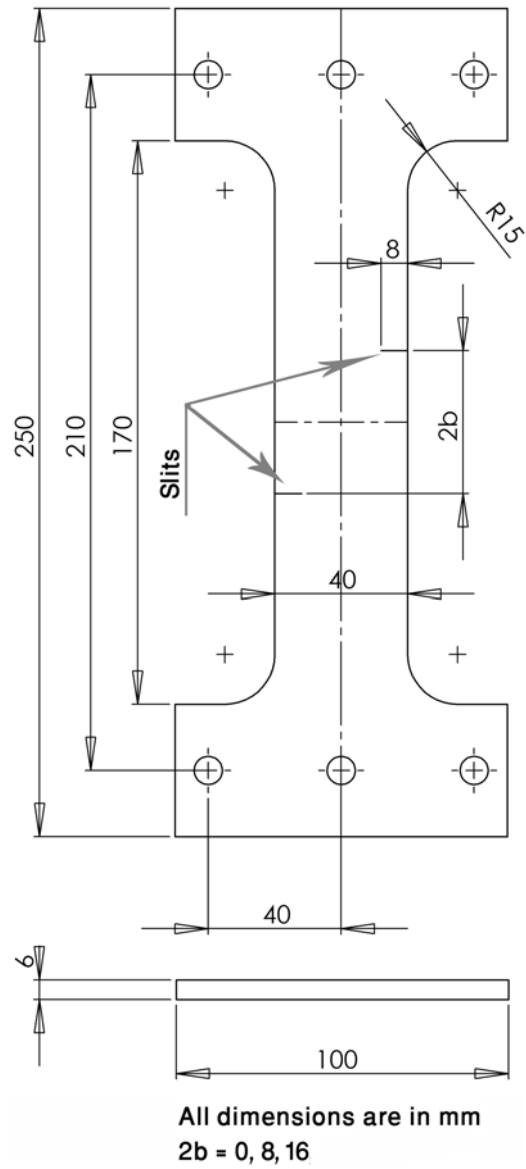
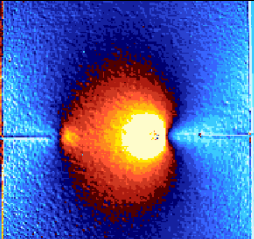
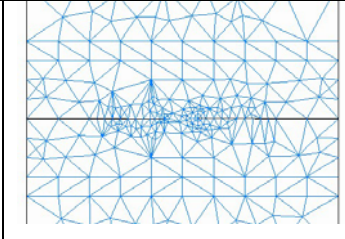
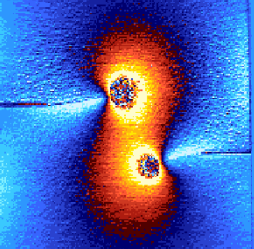
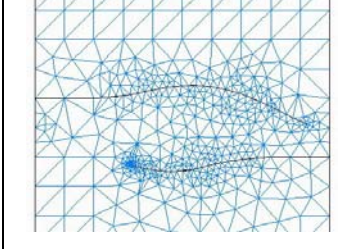
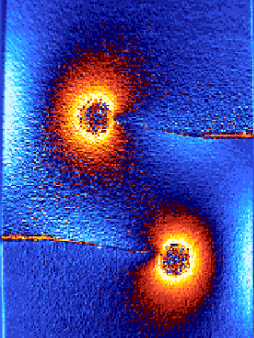
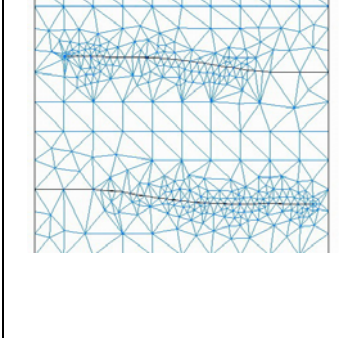
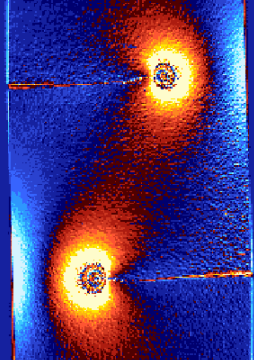
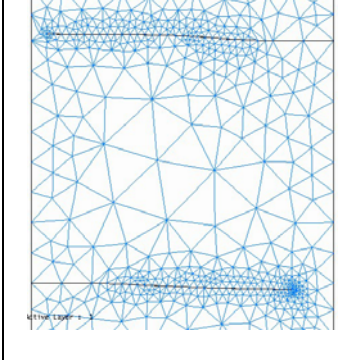


Figure 4. Design of the offset double edge slit fatigue specimens

0 mm		
8 mm		
16 mm		
32 mm		

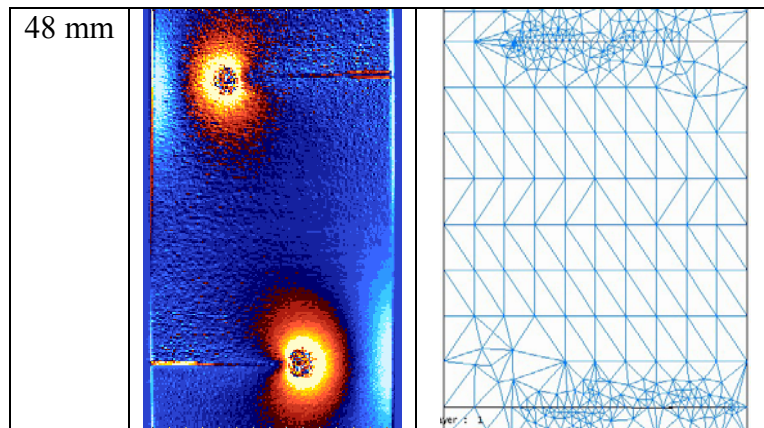
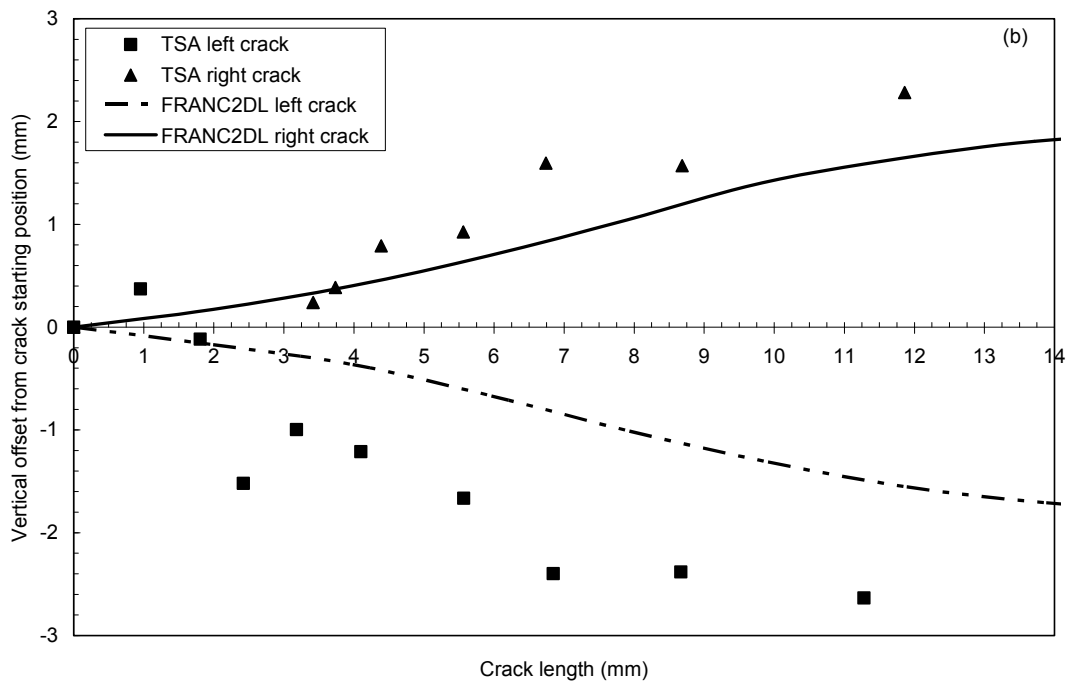
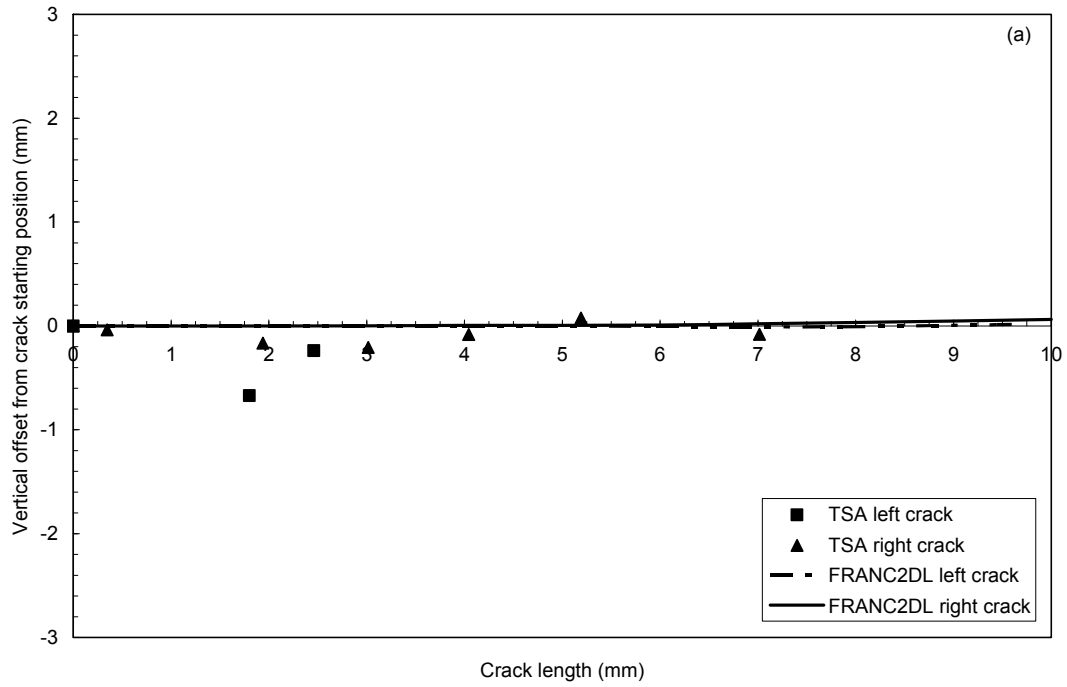


Figure 5 (top) Crack tip stress field using thermoelasticity recorded towards the end of crack growth , (bottom) final predicted paths of interacting cracks using the FRANC2DL finite element package for five different crack vertical offsets of 0, 8, 16, 32, and 48 mm.



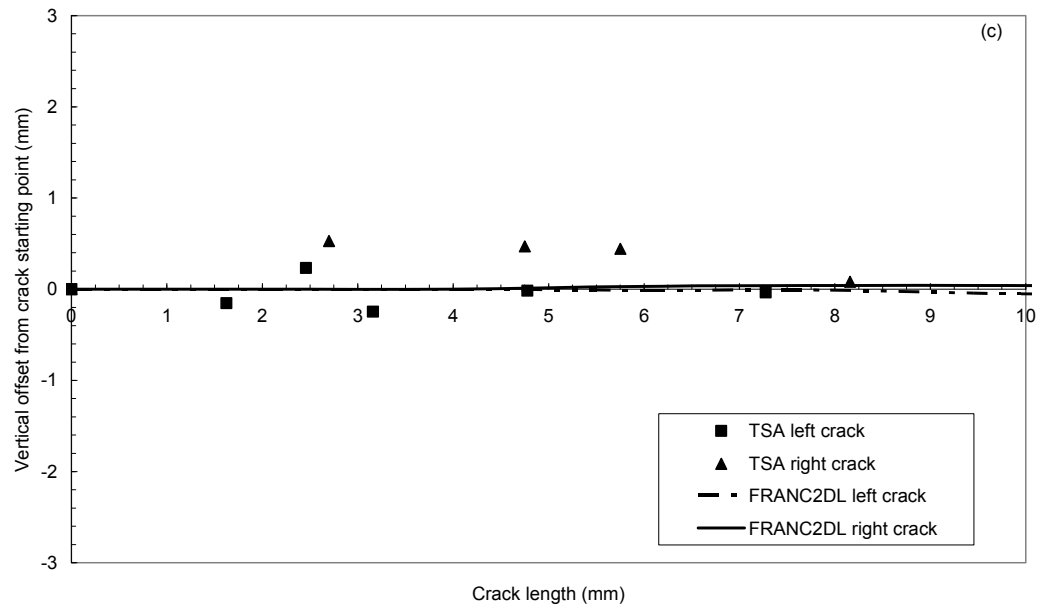
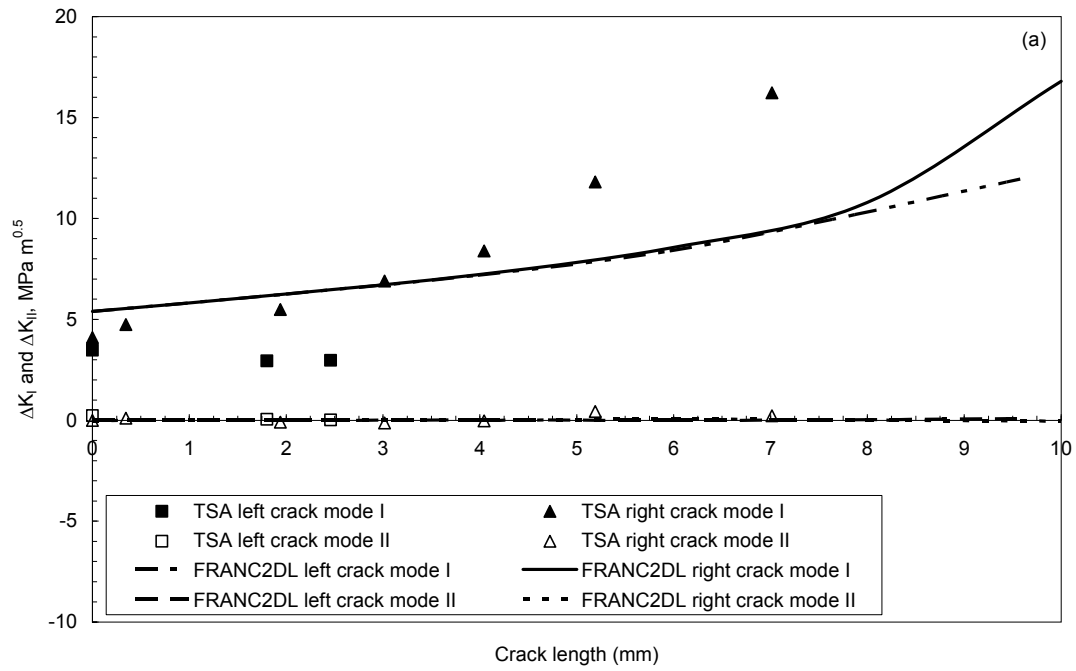


Figure 6. Left and right fatigue crack path comparison using thermoelastic stress analysis and finite element analysis (FRANC2DL). (a) 0 mm offset, (b) 16 mm offset, (c) 48 mm offset. The slit length is not included in the scale.



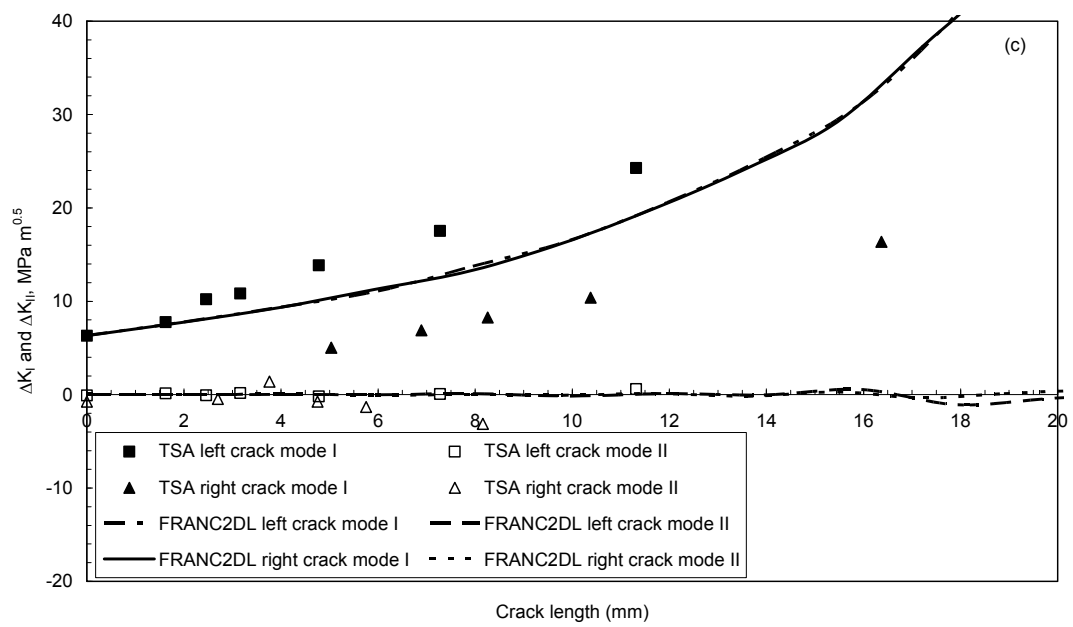
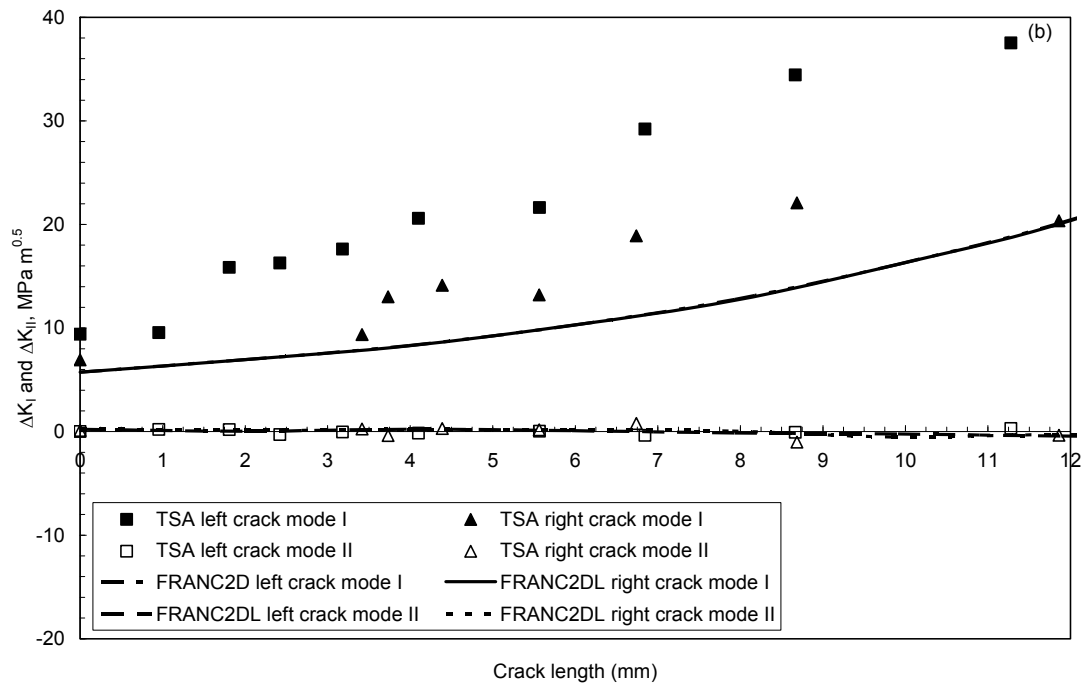


Figure 7. Left and right stress intensity factors (ΔK_I and ΔK_{II}) using thermoelastic stress analysis and finite element analysis (FRANC2DL). (a) 0 mm offset, (b) 16 mm offset, (c) 48 mm offset. The slit length is not included in the crack length scale.

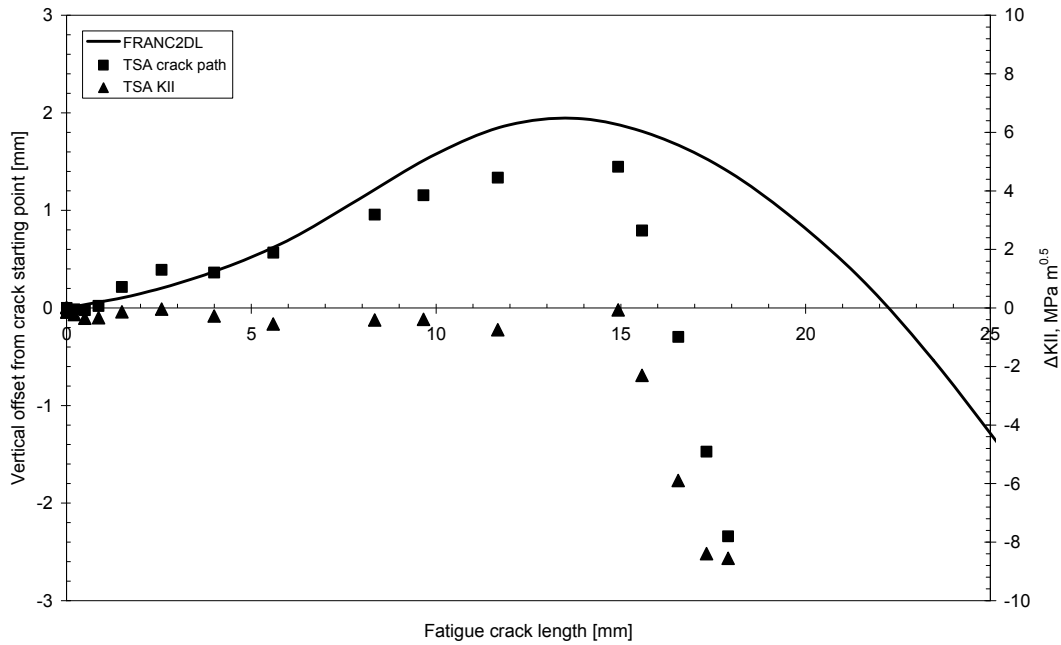


Figure 8. Fatigue crack path determined by FRANC2DL and TSA, as well as the mode II stress intensity factor determined by FATCAT for a specimen with 8 mm offset cracks. The slit length is not included in the crack length scale.

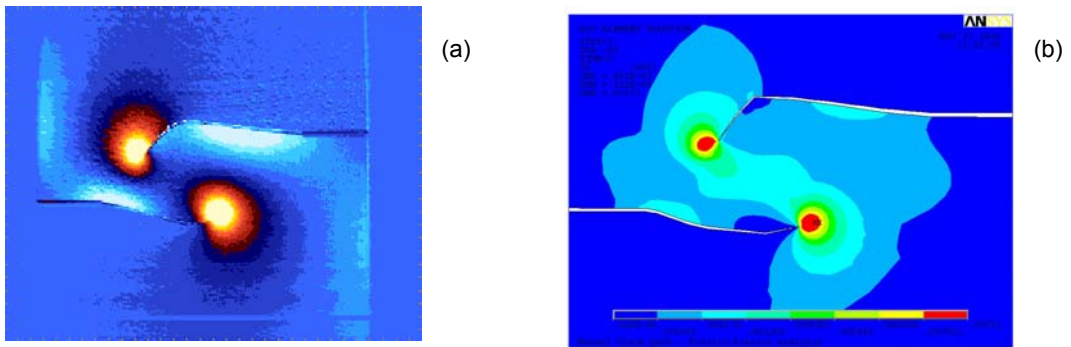


Figure 9. (a) TSA image and (b) ABAQUS non-linear FE results for a specimen with 8 mm offset cracks

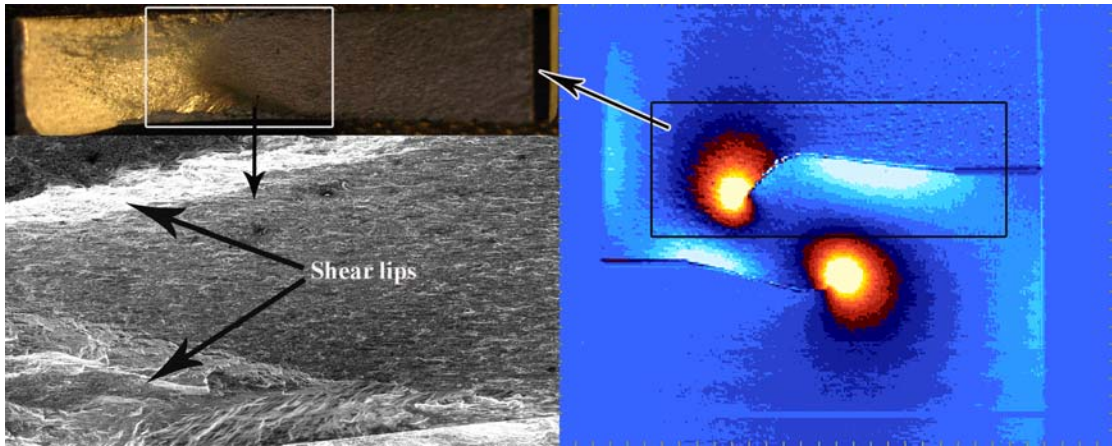


Figure 10. Fractured surface of the specimen with 8 mm offset cracks